

Negative electron affinities from conventional electronic structure methods

Kenneth D. Jordan · Vamsee K. Voora ·
Jack Simons

Received: 22 November 2013 / Accepted: 2 January 2014 / Published online: 14 January 2014
© Springer-Verlag Berlin Heidelberg 2014

Abstract If the potential V describing the interaction between an excess electron and a ground-state neutral or anionic parent is sufficiently attractive at short range, electron-attached states having positive electron affinities (EAs) can arise. Even if the potential is not attractive enough to produce a bound state, metastable electron-attached states may still occur and have lifetimes long enough to give rise to experimentally detectable signatures. Low-energy metastable states arise when the attractive components of V combine with a longer-range repulsive contribution to produce a barrier behind which the excess electron can be temporarily trapped. These repulsive contributions arise from either the centrifugal potential in the excess electron's angular kinetic energy or long-range Coulomb repulsion in the case of an anionic parent. When there is no barrier, this kind of low-energy metastable state does not arise, but improper theoretical calculations can lead to erroneous predictions of their existence. Conventional electronic structure methods with, at most, minor modifications are described for properly characterizing metastable states and for avoiding incorrectly predicting the existence of metastable states with negative EAs where no barrier is present.

Keywords Electron affinities · Metastable anions · Electron–molecule interaction potential

1 Introduction

An electron may interact with the ground state of a parent (neutral, cation, or anion) to produce an electron-attached species having a lower energy than that of the parent. Such species are said to have positive electron affinities (EAs) and occur at discrete (i.e., quantized) energies that can be found using bound-state electronic structure methods. In addition, an electron can interact with the same parent to produce a species having a higher energy than that of the parent. In fact, there exists a continuum of such states having energies $E > 0$, where $E = 0$ is taken to be the energy of the parent plus an electron infinitely far away and having zero kinetic energy.

The full treatment of the states with $E > 0$ lies within the realm of electron–molecule scattering theory. In general, continuum levels cannot be addressed using conventional electronic structure techniques. However, for circumstances discussed in this paper, the density of electron-plus-parent states $\rho(E)$ may be concentrated in certain energy ranges $E \pm \delta E$ to produce states that can be viewed as metastable with lifetimes $\delta t \approx h/\delta E$ related to the energy range δE over which the high state density exists. These states are characterized by energies E that are not rigorously quantized but can be specified within ranges δE , and they can give rise to spectroscopic features that allow them to be experimentally differentiated from the underlying continuum of states. These metastable states are associated with the negative EAs and can be identified using conventional electronic structure codes with, at most, straightforward modifications, but, as we demonstrate here,

Dedicated to Professor Thom Dunning and published as part of the special collection of articles celebrating his career upon his retirement.

K. D. Jordan · V. K. Voora
Department of Chemistry, University of Pittsburgh,
Pittsburgh, PA 15260, USA
e-mail: jordan@pitt.edu

J. Simons (✉)
Department of Chemistry, University of Utah,
Salt Lake City, UT 84112, USA
e-mail: jack.simons@utah.edu

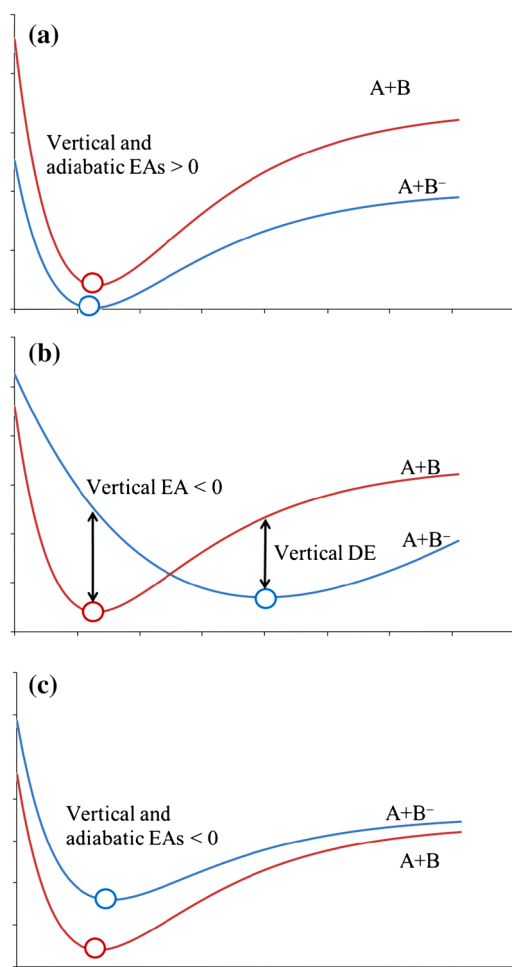


Fig. 1 Qualitative depictions of AB^- anion (blue) and AB neutral (red) potential energy curves as functions of a geometrical coordinate for three cases discussed in the text

considerable care must be used to distinguish such states with energies lying within the region $E \pm \delta E$ of high state density from states belonging to the underlying continuum whose energy can have any value $E > 0$.

Within the Born–Oppenheimer picture, the electronic stability of molecular anions depends crucially on the relative energies of the anion and neutral potential energy surfaces at various geometries. For example, an electron-attached species may have a positive EA at one geometry yet be metastable and have a negative EA at another geometry. Figure 1a depicts a case in which the anion lies below the neutral at the neutral’s equilibrium geometry (which gives a positive vertical EA) and lies below the neutral at the anion’s equilibrium geometry [producing a positive vertical detachment energy (DE)]. The adiabatic EA, defined as the energy of the neutral at its equilibrium geometry (the red circles in Fig. 1) minus the energy of the anion at its equilibrium geometry (the blue circles in Fig. 1), is positive for the case shown in Fig. 1a.

Figure 1b depicts a case where the anion lies above the neutral at the minimum of the latter (giving a negative vertical EA) and lies below the neutral at the anion’s equilibrium geometry (giving a positive vertical DE). Furthermore, the adiabatic EA is negative if the energy of the anion at its minimum lies above the energy of the neutral at its minimum as shown in Fig. 1b. Alternatively, if the minimum of the anion in Fig. 1b were lowered such that it lies below the energy of the neutral at its minimum, a positive adiabatic EA would result. Finally, Fig. 1c depicts a case in which the anion lies above the neutral at all geometries thus producing negative vertical and adiabatic EAs.

Anions with potential energy surfaces as depicted in Fig. 1b and c are unstable to electron detachment, and the plots of their energies as functions of molecular geometry should be thought of as plots of the center of the range $E \pm \delta E$ of enhanced state density. Also, the lines in such plots should be drawn with Heisenberg widths δE that vary with geometry. However, for visual clarity, the plots of potential energy curves of metastable states will, throughout this paper, be shown as simple lines.

For the case shown in Fig. 1c, the electron will undergo autodetachment at any geometry but it may have a lifetime long enough to allow it to produce a spectroscopic signature that is readily detected in laboratory experiments. For the situation illustrated by Fig. 1b, in the absence of non-Born–Oppenheimer coupling between the electronic and vibration–rotation degrees of freedom, the electron cannot detach at geometries where the anion lies below the neutral. However, if vibrational motion allows the anion to access geometries where its energy lies above the neutral, the anion of Fig. 1b can undergo detachment, in which case the rate of electron loss will depend on the rate at which such geometries are accessed. Finally, even in the case illustrated in Fig. 1a, the anion will become metastable if its level of vibrational or rotational excitation places its total energy above the zero-point level of the neutral molecule. In this case, the magnitude of vibration/rotation–electronic couplings governs the lifetime of the anion. Vibrationally/rotationally excited anions with potentials such as that shown in Fig. 1a usually have much longer lifetimes than anions with potentials as illustrated in Fig. 1c because such non-Born–Oppenheimer coupling is usually weak.

2 The physical content of electron–molecule interaction potentials

To appreciate what determines whether an anion’s electronic energy lies above or below that of its parent in its ground electronic state at a particular molecular geometry, it is important to understand the physical content of the interaction potential $V(r)$ experienced by an excess electron interacting with the parent system. A rigorous basis for

defining $V(r)$ begins with the Schrödinger equation governing the $(N+1)$ -electron wave function of the parent-plus-electron system

$$H(x, r)\Psi(x, r) = E\Psi(x, r) \\ = [H(x) + H(r) + U(x, r)]\Psi(x, r) \quad (1)$$

Here, $H(x)$ is the electronic Hamiltonian containing the kinetic energy, electron–nuclear attractions, and electron–electron interactions for the first N electrons whose coordinates collectively are denoted x ; $H(r)$ is the electronic Hamiltonian containing the kinetic energy and electron–nuclear attractions for the $N+1$ st electron whose coordinates are denoted r ; and $U(x, r)$ is the electron–electron interaction potential between the $N+1$ st electron and the parent's N electrons and is of the form $\sum_{i=1}^N \frac{e^2}{|r-x_i|}$.

At large values of $|r|$, $V(r)$ should be equal to the electrostatic potential energy of interaction of a negatively charged probe particle at r with the N -electron parent species in its ground electronic state plus the potential energy of interaction of the probe particle with the various moments it induces in the parent. For example, at large $|r|$, $V(r)$ should contain the following terms:

- Coulomb attraction (if the parent is a cation) or repulsion (if the parent is an anion),
- charge–dipole, charge–quadrupole, and higher charge–multipole interactions,
- charge-induced–dipole and higher charge-induced–multipole interactions.

In the present study, we focus on states that arise through electron attachment to the *ground state* of the parent in which case the electronic configuration $\Psi(x, r)$ of the electron-attached species can be qualitatively described as an antisymmetrized product of a wave function $\psi(x, r)$ that is an eigenfunction of $H(x) + U(x, r)$ multiplied by a spin-orbital $\phi(r)$ occupied by the excess electron $\Psi(x, r) = A\psi(x, r)\phi(r)$. The function $\psi(x, r)$ is the ground-state wave function of the parent in the presence of a stationary excess electron whose interaction with the parent is given by $U(x, r)$

$$[H(x) + U(x, r)]\psi(x, r) = E(r)\psi(x, r) \quad (2)$$

$E(r)$ is the energy of the ground-state parent as it interacts with the stationary excess electron located at r , and A is the antisymmetrizer operator.

In addition to the vibration/rotation-excited anions whose electron detachment depends on non-Born–Oppenheimer couplings discussed earlier, there is another class of metastable states that arise in anions but that also is not the focus of the present study. In these states, which are called core-excited, the excess electron is temporarily bound to an excited electronic state of the parent. There are two types of core-excited anion states [1]—those in which the anion lies

energetically above its parent and which tend to be short lived, and those that lie energetically below their parent state, and which can be quite long lived. Both types are discussed in Ref. [1] using ethylene as an example, but similar states occur in other olefins and in polyenes. In general, core-excited anions states in which the orbitals involved in the excitation and electron capture are valence, e.g., the $\pi^1 \pi^{*2}$ state of the ethylene anion, are of the former type, while anions involving excitation to and electron capture into Rydberg orbitals are of the latter type, an example of which is the $\pi^1(3s)^2$ anion of ethylene. The latter anion lies approximately 0.5 eV below the parent $\pi^1 3s^1$ Rydberg state for ethylene, and its autodetachment involves a two-electron process in which one electron is ejected from the $3s$ orbital, while another electron relaxes from the $3s$ orbital into the π orbital. The lifetimes for undergoing such two-electron events are often significantly longer than those for tunneling through the barriers arising in the states of primary interest here.

2.1 Electrostatics, polarization, antisymmetry, and orthogonality

It is possible to use perturbation theory to reduce the solution of Eq. (1) to an equation to be solved for the spin-orbital characterizing the excess electron. This results in an equation of the form

$$[H(r) + E(r) - E]\phi(r) \\ - \sum_{i=1}^N \int \psi^*(x, r)U(x, r)\psi(r_i, r)\phi(x_i)dx + V_{\text{rep}}(r)\phi(r) \\ = 0 \quad (3)$$

$H(r)$ contains the kinetic energy of the excess electron plus the electron–nuclear Coulomb interactions of this electron. $E(r)$ is, as explained earlier, the energy of the ground-state parent in the presence of a stationary excess electron at r . $E(r)$ can be expressed as the energy E_0 of the parent in the absence of the excess electron plus the sum of electrostatic $V_{\text{es}}(r)$ (e.g., Coulomb, permanent dipole, permanent quadrupole) and induced $V_{\text{ind}}(r)$ (e.g., dipole polarization, quadrupole polarization) interactions between the parent and the stationary electron as well as contributions describing non-adiabatic energies $V_{\text{non-ad}}(r)$ arising from the finite kinetic energy of the excess electron [2–4]. The terms in the sum in Eq. (3) are the exchange contributions, collectively referred to as $V_{\text{exch}}(r)$ arising from the antisymmetry of the $(N+1)$ -electron wave function. Finally, $V_{\text{rep}}(r)$ is a repulsive potential arising from the constraint that the excess electron's spin-orbital be orthogonal to the parent's wave function. In its simplest form in which $E(r)$ is approximated by Hartree–Fock (HF)-level electrostatic interactions, Eq. (3) describes the static-

exchange approximation in which $\phi(r)$ is equivalent to an unoccupied (i.e., virtual) HF orbital.

By combining $V_{\text{electrostatic}}(r) + V_{\text{induced}}(r) + V_{\text{non-ad}}(r) + V_{\text{exchange}}(r)$ with $V_{\text{rep}}(r)$, we obtain a one-electron *potential* $V(r)$ that combines with $H(r)$ to yield an equation to be solved for the excess electron's spin-orbital

$$[H(r) + V(r) - E]\phi(r) = 0 \quad (4)$$

The eigenvalues E in Eq. (4) specify the energies of the electron-attached species relative to the parent at a fixed geometry of the molecule. Negative values of E correspond to bound states, and positive values to unbound states. For bound states and metastable states, E is equal to minus the EA. Equation (4) has served as the basis for developing several one-electron models for describing excess electrons interacting with water clusters and other systems [5]. We now turn our attention to the features of the total potential $V(r)$ that combine with $H(r)$ to determine when either a positive EA or a metastable state can be expected.

2.2 Centrifugal potential contributions

For temporary anions with Born–Oppenheimer potential energy surfaces lying above the corresponding neutral's surface (as in Fig. 1c), the attractive components in $V(r)$ are not strong enough to produce a negative eigenvalue E in Eq. (4). In such cases, it is important to consider whether the repulsive angular momentum centrifugal potential arising from the kinetic energy operator $-\frac{\hbar^2}{2m}\nabla_r^2$ can combine with $V(r)$ to produce an *effective radial potential* $V_{\text{eff}}(r)$ having a barrier behind which the excess electron can be temporarily trapped. It is through such a combination of repulsive and attractive potentials that low-energy metastable anion states often arise, with the barrier and well behind it generating a high density of states in certain energy ranges.

To illustrate, consider the specific examples of placing an excess electron into the lowest unfilled valence orbital of N_2 , H_2 , H_2O , or CO_2 . In the case of N_2 , the lowest empty valence orbital is of π_g symmetry, which has a dominant component of angular momentum corresponding to the quantum number $L = 2$ (referred to as a *d*-wave in the language of electron scattering theory). The $\frac{L(L+1)\hbar^2}{2mr^2}$ centrifugal potential combines with $V(r)$ to produce an effective potential that has sizable (~ 8 eV) barrier, which results in an N_2^- anion that lives long enough to display resolvable vibrational structure in the total cross section for electron scattering even though it is unstable with respect to N_2 plus a free electron [6]. For H_2 , the lowest unoccupied valence molecular orbital (LUMO) is of σ_u symmetry and is dominated by an $L = 1$ (*p*-wave) component. This results in a lower angular momentum barrier (through

which the electron must tunnel to escape) than in N_2^- and hence a shorter anion lifetime. As a result, H_2^- appears as a broad resonance lacking resolvable vibrational structure in the electron scattering cross section [7].

In the case of H_2O , the lowest antibonding O–H σ_g^* valence orbital is of a_1 symmetry and has a large $L = 0$ component. As a result, there is no barrier behind which the excess electron can be trapped, and thus the corresponding 2A_1 state of H_2O^- is not detected experimentally. Essentially, the $a_1 \sigma_g^*$ valence orbital has dissolved in the continuum of a free electron plus the neutral molecule. Later, we will demonstrate theoretical tools for handling the metastable states of N_2^- and H_2^- and for avoiding incorrectly predicting a low-energy metastable 2A_1 state of H_2O^- to exist. It should be pointed out that there are metastable 2A_1 states of H_2O^- , but these states lie at higher energies and have orbital occupancies (e.g., $1a_1^2 2a_1^2 1b_2^2 3a_1^1 1b_1^2 4a_1^2$) in which an occupied orbital of H_2O is excited and the excess electron is attached to an excited orbital. That is, they are of the core-excited variety mentioned earlier and are not the kind of low-energy metastable states we are focusing on.

Whether an anion is stable or metastable can also depend on the geometry of the molecule. For example, the lowest-energy unoccupied valence orbital of CO_2 at the linear equilibrium structure is of π_u symmetry and thus has a nonzero centrifugal potential. As a result, a metastable anion results from electron capture into this orbital as can readily be detected in electron scattering measurements (with a peak in the cross section near 3.8 eV) [8]. However, when CO_2 is bent, the in-plane component of the π_u orbital acquires a_1 symmetry, which introduces an $L = 0$ component and lowers the centrifugal barrier and thus the anion's lifetime. The fraction of $L = 0$ character increases with increased bending, and it has been concluded that a metastable state having a lifetime long enough to be detectable occurs only for OCO angles $>165^\circ$ [9].

2.3 Differential electron correlation and problems with Hartree–Fock and DFT

There are often substantial (1–2 eV) differences between the correlation energy of a bound or metastable valence-type anion and its neutral parent. In fact, the correlation contribution to the electron binding is often of the same order of magnitude as the EA itself, so inclusion of electron correlation effects is essential for accurately characterizing these anion states. It is possible for the correlation energy of the parent to be larger than that of the anion, for example, in cases where the excess electron attaches to a vacant valence spin-orbital that contributes strongly to

electron correlation in the parent. The occupancy of this spin-orbital in the anion then excludes it from being used to correlate the anion's electrons thus reducing the anion's correlation energy. For example, in olefins, the parent's two electrons occupying π orbitals derive much of their correlation energy through double excitations of the form $\pi^2 \rightarrow \pi^{*2}$. If the π^* orbital is occupied to form the anion, the two electrons occupying the π orbital can no longer use the $\pi^2 \rightarrow \pi^{*2}$ excitation to gain correlation energy. However, it is more common for the anion to have considerably larger correlation energy than its parent neutral. In either case, it is important to include correlation effects because they often contribute a very significant percentage of the electron-binding energy.

Finally, it should be noted that in many cases, density functional theory (DFT) methods using standard GGA functionals such as B3LYP and PBE overbind anion states and can thus predict a stable anion when, in fact, the anion is metastable or there is not even a metastable anion. For example, DFT calculations performed with a flexible basis set incorrectly predict that CO₂ in its linear structure has a bound ${}^2\Sigma_g^+$ anion. This is less of a problem when using range-separated DFT methods [10] that have the correct long-range exchange interaction.

2.4 Variational collapse is a problem to be overcome

When electron correlation is ignored and the anion is treated within HF theory, a phenomenon known as variational collapse can plague the calculation as we now illustrate. For the reasons explained above, a HF-level treatment of an anion whose parent actually has a positive EA may (incorrectly) predict the anion to lie above the parent if the anion's correlation energy exceeds that of the parent. In such a situation, the HF wave function of the anion will collapse to a function describing the parent plus an approximate continuum function for the excess electron if the atomic orbital basis set has sufficiently diffuse functions in it. This happens because, within the variational HF calculation, a lower energy is achieved by forming a wave function with the $N + 1$ st electron in an orbital that is infinitely removed from the parent. Only by properly including the correlation energy of the excess electron will the energy of the anion be adjusted to lie below the energy of the parent.

It is tempting to try to avoid this variational collapse by limiting the basis set's radial extent thus not allowing the $N + 1$ st electron to escape. However, as we discuss in great detail in this paper, although this approach produces a HF state in which the excess electron remains attached to the parent, this $(N + 1)$ -electron HF wave function cannot be trusted to offer a reasonable zeroth-order function to subsequently use in a correlated

calculation. The central issue is how to limit the basis set's radial extent in a way that generates an $N + 1$ st orbital that, once electron correlation effects are added to the potential the excess electron experiences, produces a correct description of the bound excess electron. Arbitrarily limiting the basis' radial extent is not a correct approach, but the so-called stabilization methods we discuss later are.

Analogous variational collapse issues also plague calculations when attempting to identify metastable electron-attached states, even when including electron correlation effects. For example, for the case illustrated in Fig. 1c, a straightforward application of traditional electronic structure methods (even correlated methods) to the anion is guaranteed, when using a radially flexible basis set, to collapse onto the neutral plus an approximate continuum function. As discussed later, researchers have developed a variety of methods, including the stabilization method [11, 12] and the coordinate rotation method [13], for avoiding the variational collapse problem when the electron-attached species is metastable, and much of the latter part of this paper is dedicated to illustrating how to use these tools within conventional electronic structure codes.

As noted above, a HF-level description may, because of the differential correlation energy, predict a negative EA for a species that is actually bound. In such cases, if the $(N + 1)$ st HF orbital has resulted from variational collapse, using it to form a $(N+1)$ -electron wave function as a starting point for subsequent MPn or coupled cluster treatment of electron correlation is problematic. So, even though CCSD(T) often captures a large percentage of the correlation energy, if the initial approximation to the wave function has the variationally collapsed HF orbital occupied, even this powerful technique cannot be trusted. It is essential that the orbital occupied by the excess electron offer a reasonable approximation to the $(N+1)$ -electron wave function if correlated methods that use this function as their starting point are to be trusted. If the stabilization methods discussed later are used to form an initial $(N+1)$ -electron wave function, then subsequent MPn or coupled cluster treatment of electron correlation will likely be reliable.

There are methods such as Green's function [14] or EOM-CCSD [15] theory that can be especially useful in such problematic cases because their working equations can be cast in a way that does not depend on the qualitative correctness of the HF orbitals. Not only do Green's function and EOM methods provide a route for calculating EAs but they also give descriptions of the electron-parent interaction potential that can supplement the perturbation theory approach with $V(r)$ mentioned earlier. Both theories can be cast in a form [16] in which

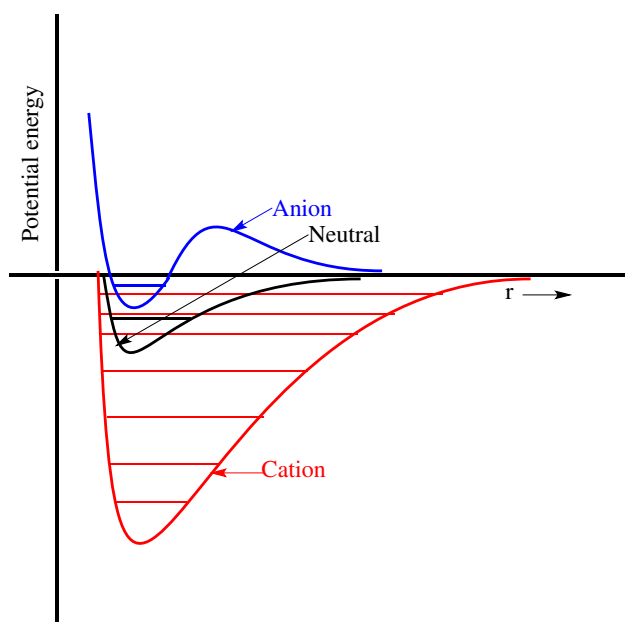


Fig. 2 Qualitative depiction of effective potentials associated with an excess electron interacting with a cation, a neutral, or an anion as a function of the distance between the electron and the parent species

the EA is obtained as an eigenvalue of a one-electron energy-dependent Hamiltonian whose matrix elements account for the excess electron's kinetic energy, its attractions to the parent's nuclei, its electrostatic and induced interactions with the parent's electron density, and the fact that the excess electron is indistinguishable from the parent's electrons (i.e., antisymmetry). The eigenfunctions of these one-electron Hamiltonians are called Dyson orbitals and are closely related to the $\phi(r)$ that we described above.

Having introduced many of the concepts and issues that arise when treating electron-attached species, we move on to address the primary purpose of this paper. It is to present approaches capable of distinguishing between metastable anions arising in regions of enhanced state density and the underlying continuum of states and to offer guidance about how to characterize the former. Before discussing these issues, it will prove useful to examine several illustrative systems to show how the electron–molecule potential and angular momentum play key roles in determining whether the electron-attached state is stable or metastable. In Sect. 3, we describe the potentials $V(r)$ and effective potentials $V_{\text{eff}}(r)$ that govern the interaction between an electron and a cation, neutral, or anion, and we illustrate features of these potentials that produce bound or metastable states. Several examples from the recent literature are used to illustrate the diverse behavior arising in these systems. In Sect. 4, we discuss theoretical tools to focus on metastable electron-attached states. Section 5 provides a summary of the main points.

3 Comparing electron–cation, electron–neutral, and electron–anion interaction potentials

As explained in Sects. 1 and 2, the ability of an atom or molecule to bind an extra electron is governed by the potential $V(r, \theta, \phi)$ between the electron and the atom or molecule. This potential depends on the location (given by the variables $r, \theta,$ and ϕ , denoted collectively as \mathbf{r}) of the electron and on the electrostatic moments and polarizabilities of the underlying parent atomic or molecular species. In Fig. 2, we give qualitative depictions of the radial behavior of $V(r, \theta, \phi)$ for three cases:

1. Interaction of an electron with a cation of charge Z to form a species with charge $Z - 1$, which relates to the formation of a neutral species if $Z = 1$ or to formation of a cation of lower charge if $Z > 1$.
2. Interaction of an electron with a neutral parent to form a singly charged anion.
3. Interaction of an electron with an anion of charge $-Z$ to form an anion of charge $-Z - 1$; if $Z = 1$, this corresponds to forming a dianion from a mono-anion.

3.1 The electron–neutral case

As illustrated in Fig. 2, the depth of the outer region potential well appropriate for an electron interacting with a neutral atom or molecule is less deep than that associated with the electron–cation interaction. The depth of the well depends on the balance between the attractive and repulsive contributions to $V(r, \theta, \phi)$. The spatial range and strength of the repulsive contributions are determined by the sizes and shapes of the parent's occupied orbitals. The relative depths of the potential wells are determined largely by the strength of the long-range attractive components of $V(r, \theta, \phi)$.

The large- r asymptotic form of the polarization potential varies as $-\alpha/2r^4$, where α is the molecular polarizability (assuming that it is isotropic). If the molecule has a permanent dipole, the corresponding electrostatic interactions dominate over the polarization interaction at sufficiently large r . For the range of multipole moments and polarizabilities found in most molecules, the charge–multipole and charge–polarization attractions are not as strong as the Coulomb attraction present in the electron–cation case. This is why the electron–cation well depth almost always exceeds the well depths for electron–neutral or electron–anion systems and is the primary reason behind the observation that electron affinities (EAs) are nearly always smaller than ionization potentials (IPs).

In addition to having a potential well less deep than for electron–cation cases, the fact that the electron–neutral potential varies at large- r as r^{-n} with $n \geq 2$ gives rise to a

qualitative change in the pattern of bound quantum states existing in such wells. It can be shown that, within the Born–Oppenheimer approximation, any species having a permanent dipole moment in excess of 1.625 D has an infinite number of bound states into which an excess electron can attach [17–21]. However, in practice, due to Born–Oppenheimer corrections, unless the dipole is very large, only the lowest of these states is significantly bound and then only if the dipole moment is in excess of ca. 2.5 D.

To summarize, the strong electron–cation Coulomb attraction at large- r gives rise to a deep potential well supporting an infinite progression of bound electronic states for an electron interacting with an atomic or molecular cation. These bound states often provide useful spectroscopic fingerprints for studying cation or neutral species because their energy spacings fall in the visible or ultraviolet regions where high-resolution and high-sensitivity light sources and detectors can be employed. In contrast, electron–neutral potentials have shallower wells and produce few, if any, significantly bound states. Moreover, even when bound excited anion states occur, their electronic excitation energies often lie in ranges where light sources and detectors are not routinely available or are of low sensitivity. Therefore, spectroscopic probes based on accessing bound excited states are generally not feasible for anions, although photoelectron spectroscopy, which requires only one bound or long-lived state, is a powerful tool.

3.2 The electron–anion case

For an electron interacting with a negative ion of charge $-Z$, there is a long-range Coulomb repulsive Ze^2/r contribution to $V(r)$. This contribution alters the energy landscape in two ways: (1) it generates the long-range repulsive Coulomb barrier (RCB) shown in Fig. 2, and (2) it shifts the electron–neutral potential upward in energy even within the regions occupied by the parent’s valence and inner-shell orbitals. Given what was said earlier about the shallowness of electron–neutral potential wells, it should therefore come as no surprise that multiply charged anions usually have only one or no bound state. As we now illustrate, such species can also have metastable states whose lifetimes depend on the height and thickness of the RCB.

In Fig. 3, we show the molecular structure of copper phthalocyanine, 3,4',4'',4'''-tetrasulfonate $[\text{CuPc}(\text{SO}_3)_4]^{4-}$ in which the tetradentate phthalocyanine ligand has four negatively charged sulfonate groups attached to its periphery and a copper atom at its center. To illustrate the range of electron-attached states that can arise in such a species, we discuss the results of photoelectron spectroscopy experiments [22].

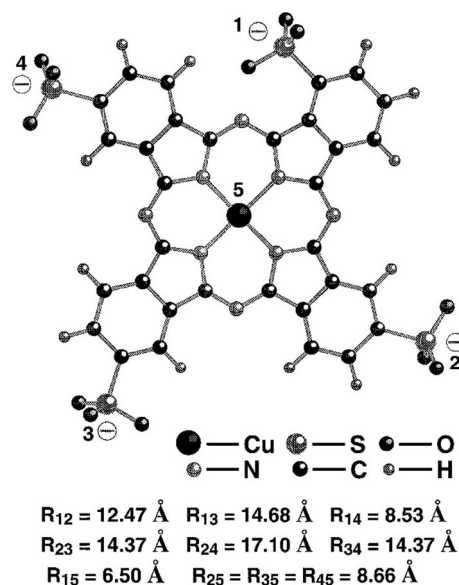


Fig. 3 Copper phthalocyanine complex with four sulfonate groups (from Ref. [22])

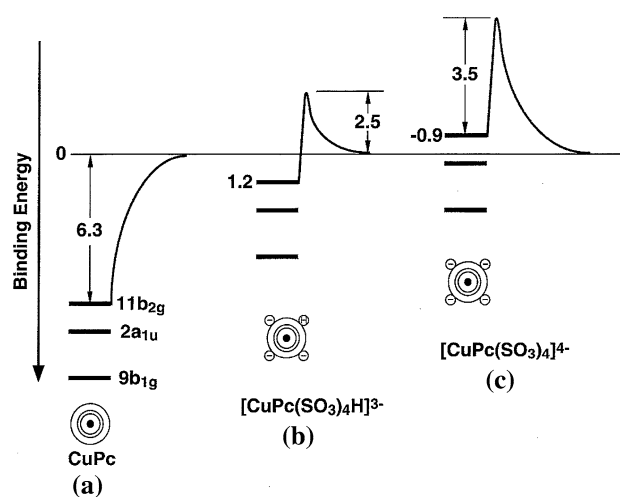


Fig. 4 Qualitative depiction of electron–parent interaction potential showing RCB and electron-binding energies for uncharged (a), triply charged (b), and quadruply charged (c) systems (taken from Ref. [22])

If the four sulfonate groups are rendered neutral and the resulting complex is subjected to photoelectron spectroscopy, it is found that the complex has an IP of 6.3 eV (the Cu-centered electron is detached). In contrast, if one of the four sulfonate groups is neutralized and the resulting triply charged anion is studied, it is found that the system has a DE of 1.2 eV [22]. However, when photons with energy only slightly higher than 1.2 eV are used, essentially no photoelectrons are ejected. Once the photon energy reaches 3.7 eV, ample electron detachment is observed and the kinetic energy of the ejected electrons is found to be ca.

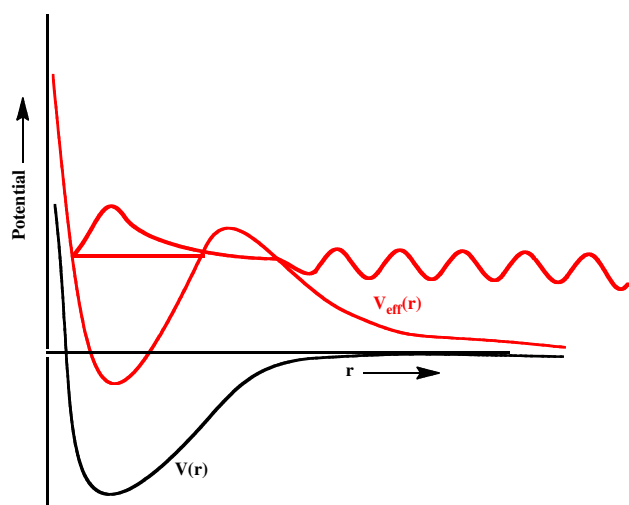


Fig. 5 Electron Mg atom potential $V(r)$ in black and effective potential $V_{\text{eff}}(r)$ in red for a nonzero value of L . The radial wave function for the $3p$ orbital producing the $3s^23p^1\ ^2P$ temporary anion is also shown

2.5 eV. It is by subtracting the kinetic energy of the electrons from the photon energy that we know the threshold detachment energy is 1.2 eV for this triply charged anion. As suggested in Fig. 4, the height of the RCB for this triply charged anion is 2.5 eV, which is why no photo-electrons are detected at photon energies below 3.7 eV.

When the quadruply charged anion having four sulfonate groups is studied, it is found that very few electrons are detached with photons having energy less than 3.5 eV. However, for photons with energy slightly greater than 3.5 eV, ample electron ejection occurs and electrons having kinetic energies of ca. 4.4 eV are detected. That is, the ejected electrons have higher kinetic energy than the energy of the photons used to eject them! This indicates that the system has a negative detachment energy value of -0.9 eV as shown in Fig. 4.

For the purposes of the present paper, the most important thing to note is that the RCB that arises in such multiply charged anions can not only lower DE values for bound electronic states but can also generate metastable states that have negative DE values, but live long enough to be experimentally detected.

3.3 More examples of metastable states

In the example just discussed, the presence of the RCB generates a potential that can bind the extra electron behind the RCB. As discussed earlier when we treated electrons interacting with N_2 , H_2 , and CO_2 , there are also situations in which the repulsive centrifugal potential generates a barrier in the effective potential that can temporarily bind an electron. To develop these ideas in more detail, let us

consider a neutral Mg atom in its ground 1S state interacting with an extra electron. Here, the electron atom potential $V(r, \theta, \phi)$ depends only on the radial coordinate r describing the distance of the electron from the Mg nucleus although the centrifugal component of the related effective potential V_{eff} also depends on the angular momentum L of the excess electron.

For this electron Mg example, $V(r)$ has a sizeable attractive component because of the significant polarizability of the Mg atom, and, when applied to s or p orbitals, it also has a short-range repulsive contribution to account for orthogonality to the Mg atom's occupied s and p orbitals. Figure 5 depicts $V(r)$ and the effective potential $V_{\text{eff}}(r)$ for a nonzero value of L .

When considering the possibility of an electron binding to the Mg atom, one needs to specify the symmetry of the electron-attached state being studied. For example, we consider the possibilities of forming a $3s^23p^1\ ^2P$ or a $3s^24s^1\ ^2S$ state. In the former case, the angular quantum number associated with the extra electron is $L = 1$; in the latter, $L = 0$ applies.

As it turns out, the e^- -Mg potential is not sufficiently attractive to support a bound state in any angular momentum channel. Thus, the $3s^24s^1\ ^2S$ state is not bound, and it is not metastable because there is no angular momentum barrier to trap the electron. However, the combination of the attractive $V(r)$ and the repulsive centrifugal potential $\frac{\hbar^2 L(L+1)}{2mr^2}$ produces an effective potential $V_{\text{eff}}(r)$ that can temporarily bind an electron to form a metastable $3s^23p^1\ ^2P$ state and is readily detected in electron scattering experiments (the anion is only 0.15 eV above the ground state of the neutral [23]). The energy level and the dominant component of the radial wave function of this metastable state are depicted in Fig. 5. In Sect. 4, we will describe how one identifies this metastable state computationally and how one should avoid incorrectly predicting that the $3s^24s^1\ ^2S$ Mg^- state is metastable.

The wave function of the metastable 2P Mg^- state has three distinct components: (1) it has a major lobe whose peak is located in the region of the minimum of $V_{\text{eff}}(r)$; (2) in the tunneling region where the energy of this state lies below V_{eff} , it decays exponentially with increasing r ; and (3) at larger r , where the energy of the state lies above V_{eff} , it displays sinusoidal variation with a de Broglie wavelength that characterizes the ejected electron's momentum. Of course, the wave function also has smaller- r components but we do not show these in Fig. 5. As detailed in Sect. 4, a proper description of the wave function in all regions is essential to achieving a full description of such metastable-state wave functions and their energies.

Unlike the Mg case just discussed, Ca has a large enough polarizability to cause its electron atom potential $V(r)$ to be sufficiently attractive to produce a $4s^24p^1$

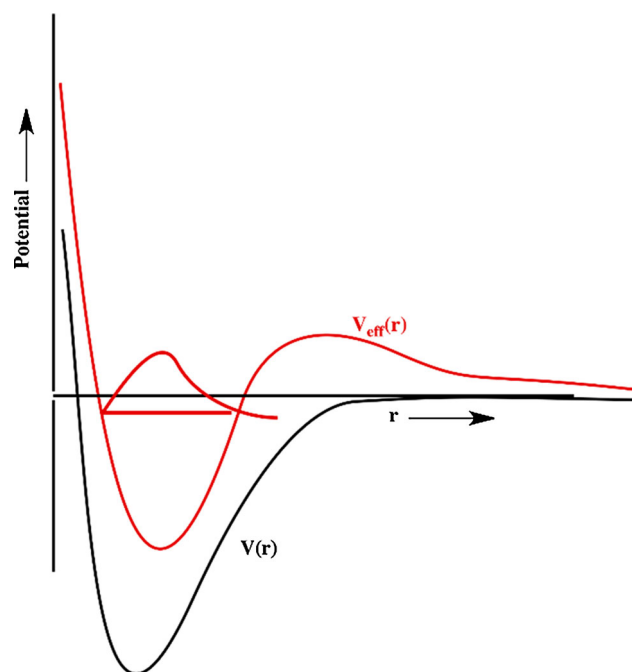


Fig. 6 Schematic of electron Ca atom effective potential (*black*) for $L = 1$ (without the centrifugal term) and the effective potential including a centrifugal potential with $L = 1$ (*red*)

2P anion state [24] that is bound by 0.025 eV. The relevant effective potential $V_{\text{eff}}(r)$ is described qualitatively in Fig. 6. In addition, Ca^- has a metastable 2D state at 0.7–1.0 eV [25, 26].

In the bound $4s^24p^1\ ^2P$ state of Ca^- , the wave function has a lobe with its maximum near the minimum of V_{eff} , and an exponentially decaying component in the region where V_{eff} is above the state's energy. However, the wave function of this bound state lacks an asymptotic sinusoidal component, which distinguishes it from the wave function of the 2P metastable state of Mg^- discussed above.

It is worth noting that the Ca atom does not form a bound $4s^25s^1\ ^2S$ anion even though it forms a bound $4s^24p^1\ ^2P$ state. The failure of Ca^- to have a bound 2S state is due to the fact that the excess electron's $5s$ orbital has to be orthogonal to the $4s$, $3s$, $2s$, and $1s$ orbitals, while the $4s^24p^1\ ^2P$ state's $4p$ orbital needs to be orthogonal to only the $3p$ and $2p$ orbitals. This offers a nice example of how orthogonality constraints contribute to the total electron–parent potential and thus affect the electron-binding energy.

In summary, an electron interacting with an alkaline earth atom may have a positive EA if V_{eff} has a sufficiently deep well as it does for $4s^24p^1\ ^2P\ \text{Ca}^-$ but not for $2s^22p\ ^2P\ \text{Be}^-$, $3s^23p^1\ ^2P\ \text{Mg}^-$, $4s^25s^1\ ^2S\ \text{Ca}^-$, or $3s^24s^1\ ^2S\ \text{Mg}^-$. Moreover, the $2s^22p^1\ ^2P\ \text{Be}^-$, $3s^23p^1\ ^2P\ \text{Mg}^-$, and $4s^24d^1\ ^2D\ \text{Ca}^-$ states exist as observable metastable states; however, the corresponding 2S anionic states are not metastable because the potentials are not sufficiently

attractive to support a bound state and there is no centrifugal barrier to radially constrain the extra electron.

4 Theoretically characterizing anions or multiply charged anions having negative EAs

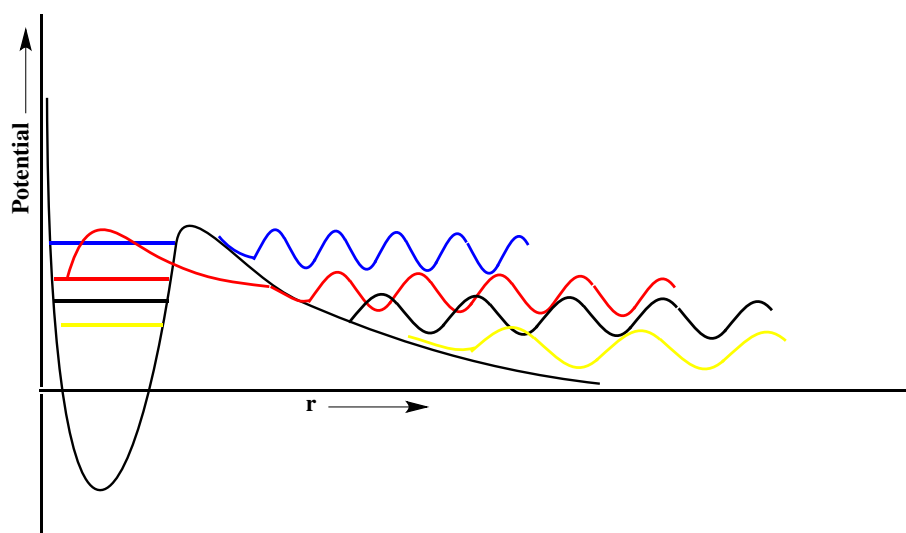
As explained in Sects. 2 and 3, a ground-state parent's electron-attached state can be metastable when the underlying parent neutral or anion presents to the approaching electron a potential $V(r)$ that is sufficiently attractive to combine with either a nonzero centrifugal potential (in the case of a neutral parent) or the repulsive Coulomb component of $V(r)$ (for an anion parent) to generate an effective potential that can bind the extra electron inside the centrifugal or Coulomb barrier. When there is no barrier present, such metastable states do not arise.

So, how does one find the metastable states and characterize their energies and lifetimes? Let us assume that one is carrying out a conventional electronic structure calculation on a system comprised of an extra electron interacting with either a neutral whose LUMO has nonzero angular momentum (and thus produces a centrifugal barrier) or anionic parent (whose RCB generates the barrier). Furthermore, let us assume that the methods being used allow one to calculate many approximate eigenvalues of the associated Schrödinger equation (e.g., within HF-based Koopmans' theorem [27] by using minus the energies of unoccupied orbitals to approximate the EAs or within configuration interaction (CI) theory by finding several eigenvalues of the $N+1$ -electron CI Hamiltonian matrix and subtracting them from the CI energy of the parent). Because such approaches utilize a finite atomic orbital basis set (which we will denote $\{\chi_J(r, \theta, \phi); J = 1, 2, \dots, N\}$), the HF orbital energies $\{\varepsilon_J\}$ or CI eigenvalues $\{E_K\}$ will be finite in number.

Because we anticipate that a true metastable state's wave function must contain a substantial component inside the barrier as well as a tunneling-range part and a large- r component that radially oscillates with a de Broglie wavelength indicative of the extra electron's asymptotic momentum, let us assume that the atomic orbital basis set consists of

1. inside-barrier and tunneling-range functions $\{\chi_J(r, \theta, \phi); J = 1, 2, \dots, n\}$ typical of a high-quality electronic structure calculation on the parent neutral or anion, augmented by
2. a set of functions $\{\chi_J(r, \theta, \phi); J = n + 1, n + 2, \dots, N\}$ that are radially more diffuse and are designed to be combined to produce functions that can oscillate radially with de Broglie wavelengths in a range that we anticipate might characterize the extra electron's asymptotic momentum.

Fig. 7 Effective radial potential (black) and wave functions of four states of the electron–parent system including a metastable state whose energy and wave function is shown in red and electron–parent collision events whose wave functions are shown in yellow, black, and blue



The primary difficulty that arises when one uses any of the approaches noted above can be illustrated using the plots of Fig. 7 where the inside-barrier and large- r components of the effective radial potential experienced by the extra electron are depicted qualitatively in black for a situation in which the limited basis set generates only a few low-energy states having $E > 0$.

Using a modest basis set, one might find among the four lowest eigenvalues (i.e., by either subtracting CI eigenvalues of the electron–parent system from the CI energy of the parent or using the negative of the HF unoccupied orbital energies) for this simple example

1. A lowest eigenvalue (denoted by the yellow horizontal line in Fig. 7) whose wave function (also in yellow) has little, if any, inside-barrier component and is dominated by a long de Broglie wavelength function existing at large- r but extending outward only as far as the most diffuse atomic basis function in $\{\chi_J(r, \theta, \phi); J = n + 1, n + 2, \dots, N\}$ allows;
2. a higher-energy eigenvalue (black) whose wave function also has little inside-barrier component, exists primarily at large- r , but has a somewhat shorter de Broglie wavelength than the first eigenfunction;
3. an eigenvalue (red) whose wave function has both a large inside-barrier component and an oscillating large- r component whose de Broglie wavelength gives the asymptotic momentum of the extra electron.
4. a fourth eigenvalue (blue) of even higher energy whose wave function is similar in character with the wave functions indicated by yellow and black curves but has a shorter de Broglie wavelength.

The wave function shown in red and its energy correspond to the metastable state. The yellow, black, and blue curves describe the extra electron with various asymptotic

kinetic energies encountering and reflecting off of the barrier on the electron–parent effective potential. It is important to note that the metastable state of interest is by no means the lowest-energy state. Moreover, as more and more diffuse basis functions are utilized in the calculation, there is an increasing number of continuum-dominated states lying below (and above) the resonance state.

It might seem possible to simply carry out a conventional quantum chemistry calculation with a reasonable number of diffuse basis functions and visually examine the inside-barrier, tunneling, and asymptotic character of many of the resulting wave functions to find the metastable state. However,

1. when studying electrons interacting with large molecules, it is extremely difficult to examine pictorially a large number of the low-energy wave functions of the electron–parent system, and, more importantly,
2. one often finds that two or more of the eigenfunctions possess substantial components of inside-barrier, tunneling, and asymptotic character. Obviously, a method is needed that can isolate the correct state when mixed states occur.

4.1 The orbital exponent stabilization method

The so-called stabilization method [11, 12] provides a means of identifying the resonances. There are multiple variants of the stabilization method, and here, we consider only the exponent scaling approach where the radial character of the diffuse basis functions is tuned by scaling their orbital exponents. If the $(N-n)$ diffuse functions $\{\chi_J(r, \theta, \phi); J = n + 1, n + 2, \dots, N\}$ are of Gaussian form, the scaling is accomplished by multiplying each of their orbital exponents by a positive scaling factor α

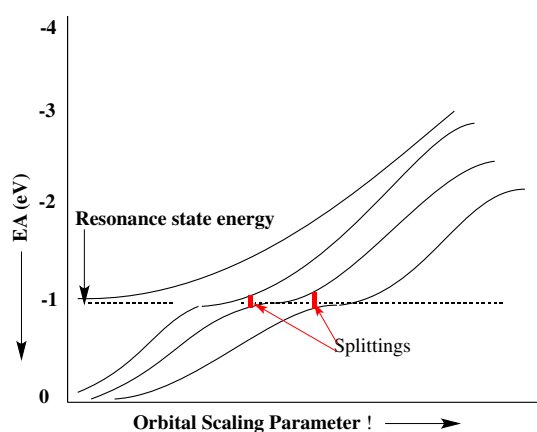


Fig. 8 Example of a stabilization calculation plot showing four $E > 0$ eigenvalues as a function of the orbital scaling parameter α , illustrating the avoided crossings that result due to the presence of a metastable state

(i.e., $\zeta \rightarrow \alpha\zeta$) ranging from less than 1.0 to larger than 1.0 (the range of α -values necessary to realize the avoided crossings discussed below varies from case to case; sometimes it can be from 0.9 to 1.2, and other times it can be from 0.5 to 1.5).

In a stabilization study in search of metastable states for electron–neutral or electron–anion systems, one carries out a series of calculations for different α values for the approximate EAs using a specified set of valence and diffuse atomic basis functions. In each such calculation, one generates approximations to several (four in the example shown in Fig. 7) approximate EAs. One then plots the lowest several approximate EAs as functions of this scaling factor and obtains a stabilization plot such as that depicted in Fig. 8.

The eigenvalues associated with continuum levels move upward in energy as α is increased because increasing α contracts the radial extent of the diffuse functions, in effect reducing the radial “box size” that confine the functions. However, if a metastable state exists, one also finds a series of avoided crossings as seen in Fig. 8. This behavior results from the coupling of (1) one state that, in a diabatic sense, contains primarily inside-barrier and tunneling-range components and whose energy is relatively insensitive to α to (2) other states having nearly the same energy but containing primarily large- r oscillatory character. One can estimate the energy of the metastable anion state as the average of the energies of the two states undergoing avoided crossing at the value of α where their energy gap is smallest. Such metastable states are often called resonance states.

In the example shown in Fig. 8, there is more than one avoided crossing near $EA = -1$ eV. A series of avoided crossings is generated as increasing α radially constrains all

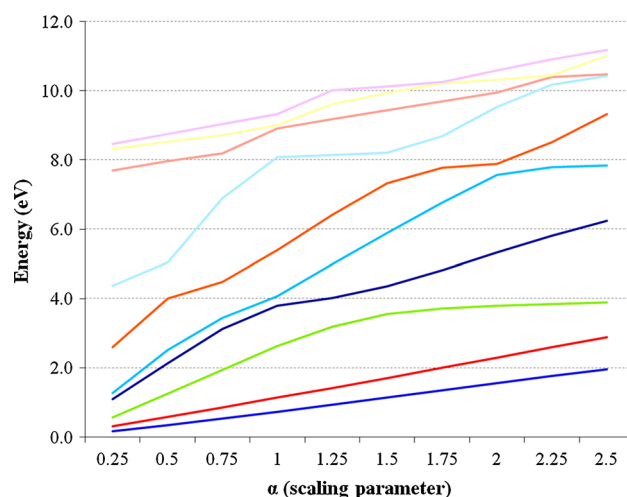


Fig. 9 Stabilization plot of the EA-EOM-CCSD energies (n.b., the EAs are minus the energies at which avoided crossings occur) for ten states of e symmetry ($L = 1$; $M = \pm 1$) for $\text{CH}_3\text{CN} + e$; the energies are given relative to that of the parent CH_3CN molecule

of the diffuse basis functions. To successfully carry out this kind of stabilization calculation, one does not need to use a basis with a large number of diffuse functions that leads to several avoided crossings. In general, it is adequate to employ a basis capable of generating only one large- r -dominated function that undergoes an avoided crossing between the inside-barrier and tunneling-range functions as α is varied.

In Fig. 9, we show a stabilization plot obtained from EA-EOM-CCSD [15] calculations on an excess electron interacting with a $\text{H}_3\text{C}-\text{CN}$ molecule, within C_{3v} symmetry with the two carbon atoms and one nitrogen atom on the z -axis, for states of e symmetry (chosen because the valence π^* orbital is of this symmetry). The basis set used to obtain these data was of 6-31+G* [28] quality with an additional set of diffuse $2s$ and $2p$ functions employed on the heavy atoms. The exponents of these supplemental s and p functions (0.0146 on C and 0.0213 on N) and of the most diffuse p functions in the 6-31+G* basis were simultaneously scaled.

In this system, the stabilization plot predicts there to be one metastable state with a negative EA of about -4 eV and another around -8 eV. By examining the character of the occupied orbitals in these two states (i.e., plotting the orbitals), we find the wave function for the lower energy resonance has significant weight from the $\text{C} \equiv \text{N}$ π^* valence orbital, whereas the higher-energy resonance is associated primarily with the electron being attracted to the dipole moment’s positive regions near the methyl group. It should be mentioned that CH_3CN also has a dipole-bound state having $E < 0$ (that we have not treated here), so this species displays both bound and metastable valence anionic states.

4.2 Lifetime estimates

From the avoided crossing in a stabilization plot, it is also possible to estimate the lifetime τ of the metastable state or the rate at which this state undergoes autodetachment

$$\text{Rate} = \frac{1}{\tau} \quad (5)$$

if tunneling through the barrier is the rate-determining factor as it is for the anion states treated in this paper. To do so, one finds the minimum in the energy splitting (see Figs. 8, 9) that occur at the avoided crossings of the stabilization plot and uses the Heisenberg relation

$$\delta E \approx \frac{h}{\tau} \quad (6)$$

with δE taken as 1/2 the minimum splitting, to determine τ . For example, the resonance at ca. 4 eV in Fig. 9 has $\delta E \approx 0.2$ eV, which corresponds to a lifetime of ca. 2×10^{-14} s. It is clear from Fig. 9 that the splitting value is not the same at each avoided crossing of the resonance near 4 eV, so there clearly is uncertainty in the lifetime thus deduced, but this is one of the simplest routes for estimating such decay rates of metastable electron-attached species. A more rigorous approach is to analytically continue the calculated energies into the complex plane and to identify the complex stationary point [29] at which $\partial E/\partial \alpha = 0$. A good example of applying this kind of stabilization method to N_2^- and Mg^- is given in Ref. [30].

4.3 The charge stabilization method

There is another stabilization-based method for estimating the energies of metastable states that is even more straightforward to implement than the exponent scaling stabilization method outlined above. Its potential for efficiency derives from the fact that it does not require the evaluation of two-electron integrals at numerous α -values, which the orbital scaling method does. It involves only modification of the one-electron components of the electronic Hamiltonian. We illustrate this so-called charge stabilization method [31] using the sulfate dianion SO_4^{2-} as an example. Here, we anticipate either being able to bind an electron to the SO_4^{1-} ion (if the attractions are strong enough) or being able to form a metastable dianion in which the electron is trapped behind the RCB of the SO_4^{1-} anion.

Our goal is to compute the EA for binding a second electron to the SO_4^{1-} anion to form the sulfate ion, and let us assume we know the equilibrium S–O bond length of this dianion. A straightforward calculation (e.g., using HF, CI, or other ab initio approach) finds that there is no state of the dianion that lies below the energy of the SO_4^{1-} ion.

That is, we find that sulfate is not electronically stable as an isolated species. So, we are faced with finding a metastable state of the sulfate dianion in which the RCB or a centrifugal potential traps the electron.

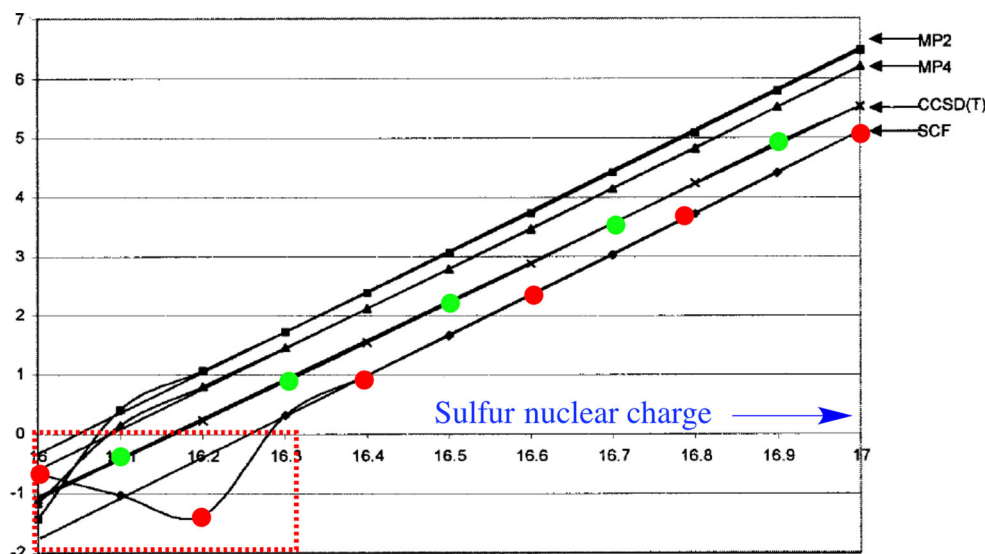
One could, of course, carry out an exponent scaling stabilization calculation on this system much like we described earlier. Alternatively, one can do the following:

1. Increase the nuclear charge of the sulfur atom from 16 to $16 + \delta q$ using a series of fractional positive values of δq . If δq were allowed to assume the value 1.0, one would be studying the ClO_4^{1-} system (at the geometry of SO_4^{2-}) rather than SO_4^{2-} and ClO_4 is known to have a positive EA. So, for some fractional positive value of δq , the EA must evolve from negative (for SO_4^{1-}) to positive (for ClO_4). Alternatively, one could increase the nuclear charges of the four oxygen atoms each by an identical small amount. Any such change to the attractive potential experienced by the excess electron that preserves the symmetry of the parent can be used.
2. Compute the EA of the fictitious XO_4^{1-} anion (where X is undergoing transmutation from S to Cl) using a good quality inside-barrier and tunneling-range atomic orbital basis and a reliable method, but only use the resultant data for values of δq for which the EA remains positive. For positive values of EA, the results of such standard electronic structure calculations can be trusted, but it is important to keep in mind the warnings issued earlier (e.g., HF may give a negative EA when; in fact, the true EA is positive and included electron correlation is usually important because of the large differential correlation energy that usually occurs).
3. Then, plot the positive EA values as a function of the increased charge δq and extrapolate the data to $\delta q \rightarrow 0$, making sure to use only data from δq values for which EA is positive. The value obtained from this extrapolation gives the estimate of the metastable state's negative EA.

An example of such a charge stabilization plot for the SO_4^{1-} system is shown in Fig. 10 with EA data obtained from HF, MP2, MP4, and coupled cluster calculations [32].

Notice that the computed data points corresponding to negative EA values (see those within the red box in Fig. 10) do not fall on the linear fits that are obtained using those data points for which EA is positive, which is why we do not use these data points in making our estimate of the actual negative EA. These energies relate to states that are part of the $\text{SO}_4^- + e^-$ continuum and become less reliable for characterizing SO_4^{2-} as δq decreases below ca. 0.25. The HF-level data deviate most strongly from the linear fit, with the MP2 and MP4 data deviating less and the CCSD(T) data deviating only slightly. In these calculations, the radial

Fig. 10 Charge stabilization plot for the electron SO_4^{1-} system computed at various levels of theory (adapted from Ref. [32]). The HF-level data follow the red dots, while the CCSD(T) data follow the green dots



extent of the basis set limits the degree of variational collapse that the $(N+1)$ st electron's orbital can undergo. As a result, this orbital retains much valence character, which, in turn, allows the correlation calculations to be reasonably successful even for $\delta q < 0.25$.

The charge stabilization method outlined above does not provide a direct estimate of the lifetime, unlike the exponent scaling stabilization method. However, other workers [33, 34] have extended this kind of approach (i.e., scaling the nuclear charge) employing non-analytic functional forms (e.g., including terms such as $(Z - Z_C)^{3/2}$) for how the EA should scale with nuclear charge Z . In that work, the $N+1$ to N -electron energy gap ΔE for values of Z for which the energy difference is real was fit to, for example,

$$Z^2 \Delta E = a + b(Z - Z_C) + c(Z - Z_C)^2 + d(Z - Z_C)^{3/2} \quad (7)$$

This fit was then used to predict the energy gap for values of $Z < Z_C$ where ΔE has a negative real part (corresponding to a metastable state) and a nonzero imaginary component (inversely related to the lifetime). Such an approach was used [33], for example, to extrapolate from the IP of Ne ($Z = 10$), through the IP of F^- ($Z = 9$), to predict the negative EA of O^- (-5.38 eV) and the lifetime (5×10^{-16} s) of O^{2-} .

It is interesting to point out that the experimental community employs “tricks” similar to the charge stabilization device to estimate negative EAs of metastable anions. For example, we show in Fig. 11 a plot of the measured electron-binding energies for sulfate anions solvated by various numbers of water molecules [35].

When sulfate is solvated by three or more water molecules, the resulting complex has a positive electron-binding energy; when two or fewer water molecules are present, the

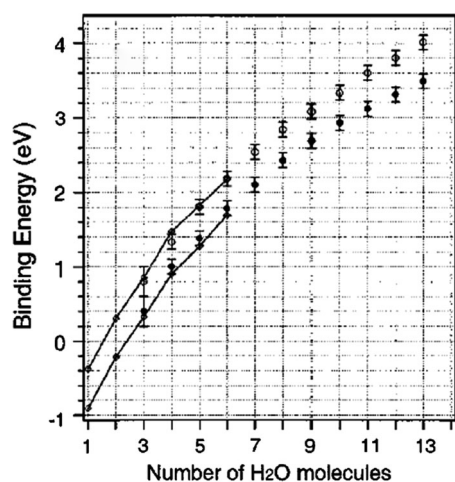


Fig. 11 Plot of the electron-binding energies, determined by photoelectron spectroscopy in Ref. [35] for $(\text{SO}_4^{2-})(\text{H}_2\text{O})_n$ clusters with $n = 13$. The lower data points relate to adiabatic electron detachment, and the upper points to vertical detachment

species is metastable. By plotting the electron-binding energy as shown in Fig. 11 and using only data points for which the complex is stable, the authors of Ref. [35] could extrapolate to predict a negative EA for SO_4^- ; doing so, we obtain an EA of -0.5 to -1.0 eV, although the data points in Fig. 11 clearly do not follow a straight line near $n = 3$, so there is considerable uncertainty in this extrapolation. These extrapolated values are in reasonable agreement with the CCSD(T) extrapolation shown in Fig. 10.

5 Summary

By analyzing the various components contributing to the interaction potential between an excess electron and a

ground-state parent that is either a neutral (forming an anion daughter) or an anion (forming a multiply charged anion), we have illustrated that several outcomes can arise.

1. The electron–parent attractive interactions may be strong enough to produce a *bound state* in which the electronic energy of the daughter lies below that of the parent, at least near the minimum energy geometry of the daughter. These cases are characterized by *positive EAs*. The ground electronic states of $\text{Ca}^-(^2P)$, Cl^- , OH^- , $\text{O}_2^-(\text{H}_2\text{O})_4^-$, $[\text{CuPc}(\text{SO}_3)_4]^{3-}$, and of the dipole-bound NC-CH_3^- provide examples of such cases. Electronic structure methods that do not involve stabilization-type analyses can be used to determine the positive EAs associated with this class of anions. However, one must employ basis functions diffuse enough to accommodate the excess electron and one should use an approach that includes electron correlation corrections because of the large correlation energy difference between the parent and electron-attached systems. Moreover, if the excess electron is not bound in the HF approximation, as is the case for $\text{Ca}^-(^2P)$, one must use electronic structure methods that do not depend on the suitability of the HF wave function (or its orbitals and orbital energies) so as to avoid the plague of variational collapse.
2. The electron–parent attractive interactions may not be strong enough to produce a bound state having a positive EA but may, in combination with either a repulsive centrifugal or a repulsive Coulomb potential, produce an effective potential having a barrier that can trap the excess electron behind it. In these cases, a low-energy *metastable electron-attached state* having a *negative EA* can form. The lifetimes of such states are governed primarily by the rate at which the excess electron tunnels through the barrier behind which it is trapped. The low-energy metastable states of $\text{Mg}^-(^2P)$, N_2^- , C_6H_6^- , SO_4^{2-} , PO_4^{3-} , $[\text{CuPc}(\text{SO}_3)_4]^{4-}$ give examples of such states. To properly characterize this class of anions, one should employ an approach that avoids the variational collapse that would otherwise occur when using diffuse basis functions capable of describing the long-range character of the metastable state's wave function.
3. If the electron–parent attractive potential is weak and if there is no repulsive Coulomb or centrifugal potential with which it can combine to form a barrier, then no low-energy electron-attached metastable state can be formed. Calculations on such systems using finite basis sets may produce energies for the electron-attached species that lie above the energy of the parent, but these are *not metastable states*. Their nature can be uncovered by improving the basis sets (especially by

enhancing the radial range of the diffuse functions) upon which the state will collapse to a function describing the parent plus the excess electron far away (i.e., not attached at all). In a stabilization calculation, one will find that the stabilization plot has no regions of avoided crossing within which inside-barrier and large- r -dominant functions are coupled. The $\text{Ca}^-(4s^25s^1) ^2S$ state provides an example of such a case.

The class of metastable electron-attached states focused on in this paper are often studied experimentally using so-called electron transmission spectroscopy (ETS) methods in which the intensity of a beam of electrons either transmitted through or scattered from a gas-phase sample is monitored as a function of the kinetic energy of the incident electrons and the kinetic energy of the scattered electrons. Low-energy shape resonance states as studied here are detected, for example, by observation of attenuation of the incident beam within a range of electron kinetic energies $E \pm \delta E$. The center of this range is used to specify the energy of the metastable state and the spread δE over which attenuation is observed is used to specify the state's lifetime via. Eq. (6). Reference [36] provides a good overview of how ETS has been used to characterize many low-energy shape resonance states of organic molecules. Typically, ETS measurements have instrumental resolutions of ca. 0.05 eV. The shape resonance states discussed here often have lifetimes in the 10^{-14} s range, which gives them Heisenberg widths δE of ca. 0.5 eV. The core-excited electron-attached states mentioned earlier in this paper, which require two-electron transitions to undergo electron detachment, have longer lifetimes and thus produce ETS signatures that have much smaller δE values. These order-of-magnitude estimates of the experimental resolution and of lifetimes and widths of metastable states offer some guidance about what accuracy one needs in determining the EAs corresponding to these states.

Acknowledgments K.D.J. acknowledges the support of Grant CHE1111235 from the National Science Foundation.

References

1. Love DE, Jordan KD (1995) Electron impact excitation of the singlet and triplet $B_{1u} \pi \pi^*$ states of ethylene near threshold. *Chem Phys Lett* 235:479–483
2. Callaway J, LaBahn RW, Pu RT, Duxler WM (1968) Extended polarization potential: applications to atomic scattering. *Phys Rev* 68:12–21
3. Kunc JA (1999) Low-energy electron–atom scattering in a field of model potentials. *J Phys B* 32:607–619
4. LaBahn RW, Callaway J (1966) Elastic scattering of low-energy electrons from atomic helium. *Phys Rev* 147:28–40

5. Voora VK, Ding J, Sommerfeld T, Jordan KD (2012) A self-consistent polarization potential model for describing excess electrons interacting with water clusters. *J Phys Chem B* 117:4365–4370
6. Schulz GJ (1973) Resonances in electron impact on diatomic molecules. *Rev Mod Phys* 45:423–486
7. Ehrhardt H, Langhans L, Linder F, Taylor HS (1968) Resonance scattering of slow electrons from H₂ and CO angular distributions. *Phys Rev* 173:222–230
8. Sanche L, Schulz GJ (1973) Electron transmission spectroscopy: resonances in triatomic molecules and hydrocarbons. *J Chem Phys* 58:479–493
9. Rescigno TN, Byrum DA, Isaacs WA, McCurdy CW (1999) Theoretical studies of low-energy electron-CO₂ scattering: total, elastic, and differential cross sections. *Phys Rev A* 60:2186–2193
10. Savin A (1996) Recent developments and applications of modern density functional theory. Elsevier, Amsterdam, p 327
11. Taylor HS (1970) Models, interpretations, and calculations concerning resonant electron scattering processes in atoms and molecules. *Adv Chem Phys* 18:91–147
12. Hazi AU, Taylor HS (1970) Stabilization method of calculating resonance energies: model problem. *Phys Rev A* 1:1109–1120
13. Moiseyev N, Certain PR, Weinhold F (1978) Complex-coordinate studies of helium autoionizing resonances. *Inter J Quantum Chem* 14:727–736
14. Schirmer J, Cederbaum LS, Walter O (1983) New approach to the one-particle Green's function for finite Fermi systems. *Phys Rev A* 28:1237–1259
15. Nooijen M, Bartlett RJ (1995) Equation of motion coupled cluster method for electron attachment. *J Chem Phys* 102:3629–3647
16. Simons J (2005) Equations of motion (EOM) methods for computing electron affinities and ionization potentials. In: Dykstra CE, Frenking G, Kim KS, Scuseria G (eds) *Theory and applications of computational chemistry: the first 40 years, a volume of technical and historical perspectives*, chap 17. Elsevier, pp 443–461
17. Jordan KD (1979) The early history of the study of electrons binding to dipoles is overviewed. *Negat Ion States Polar Mol Acc Chem Res* 12:36–42
18. Wang F, Jordan KD (2003) Theory of dipole-bound anions. *Ann Rev Phys Chem* 54:367–396
19. Garrett WR (1970) Critical binding of an electron to a non-stationary electric dipole. *Chem Phys Lett* 5:393–397
20. Garrett WR (1971) Critical binding of an electron to a rotationally excited dipolar system. *Phys Rev A* 3:961–972
21. Crawford OH (1968) Electron collision frequencies in water vapor. *Chem Phys Lett* 2:461–463
22. Wang L-S, Wang X-B (2000) Probing free multiply charged anions using photodetachment photoelectron spectroscopy. *J Phys Chem A* 104:1978–1990
23. Burrow PD, Michejda JA, Comer J (1976) Low-energy electron scattering from Mg, Zn, Cd and Hg: shape resonances and electron affinities. *J Phys B Atom Mol Phys* 9:3225–3236
24. Petrunin VV, Andersen HH, Balling P, Andersen T (1996) Structural properties of the negative calcium ion: binding energies and fine-structure splitting. *Phys Rev Lett* 76:744–747
25. Johnston AR, Burrow PD (1979) Temporary negative-ion formation in calcium vapor. *Bull Am Phys Soc* 24:1189
26. Romanyuk NI, Shpenik OB, Zapesochnyi IP (1980) Cross sections and characteristics of electron scattering by calcium, strontium, and barium atoms. *JETP Lett* 32:452–455
27. Koopmans T (1934) Über die Zuordnung von Wellenfunktionen und Eigenwerten zu den Einzelnen Elektronen Eines Atoms. *Physica* 1:104–113
28. Krishnan R, Binkley JS, Seeger R, Pople JA (1980) Self-consistent molecular orbital methods. XX. A basis set for correlated wave functions. *J Chem Phys* 72:650–654
29. Simons J (1981) Resonance state lifetimes from stabilization graphs. *J Chem Phys* 75:2465–2467
30. Chao JS-Y, Falcetta MF, Jordan KD (1990) Application of the stabilization method to the N₂⁻(²Π_g) and Mg⁻(²P) temporary anion states. *J Chem Phys* 93:1125–1135
31. Nestmann B, Peyerimhoff SD (1985) Calculation of the discrete component of resonance states in negative ions by variation of nuclear charges. *J Phys B* 18:615–626
32. Whitehead A, Barrios R, Simons J (2002) Stabilization calculation of the energy and lifetime of metastable SO₄²⁻. *J Chem Phys* 116:2848–2851
33. Herrick DR, Stillinger FH (1975) Energy and lifetime of O²⁻ from analytic continuation of isoelectronic bound states. *J Chem Phys* 62:436–4365
34. Sergeev A, Kais S (2001) Resonance states of atomic anions. *Inter J Quantum Chem* 82:255–261
35. Wang X-B, Nicholas JB, Wang L-S (2000) Electronic instability of isolated SO₄²⁻ and its solvation stabilization. *J Chem Phys* 113:10837
36. Jordan KD, Burrow PD (1987) Temporary anion states of polyatomic hydrocarbons. *Chem Rev* 87:557–588